

Retrieving the Balanced Winds on the Globe as a Generalized Inverse Problem

Huei-Iin Lu^{*,1} and Franklin R. Robertson[†]

**Universities Space Research Association, Huntsville, Alabama; and †Marshall Space Flight Center, Huntsville, Alabama*

Received July 6, 2000; revised January 30, 2001

A generalized inverse technique is applied to retrieve two types of balanced winds that characterize the large-scale dynamics of the atmosphere: rotational winds based upon the linear balance equation and divergent winds based upon the vorticity budget equation. Both balance equations are singular at or near the equator. The balance equations are transformed in spherical harmonic function space to an underdetermined system, for which the scale-weighted, least-squares solution consists of a sum of principal and singular components. The principal components represent the response to the source function for the regular eigenmodes, while the singular components are determined by the projection of an independent measurement on the singular eigenmodes. The method was tested with the NCEP/NCAR reanalysis data in which a quasi-balance condition exists. A realistic balanced wind field is retrievable when the singular components are computed based upon the reanalyzed wind data. © 2001 Academic Press

Key Words: linear balance equation; vorticity budget equation; χ problem; tropical singularities; generalized inversion; pseudo inversion; minimum-length solution; constrained linear inversion; similarity transformation.

1. INTRODUCTION

The linear balance equation (LBE) describes the geostrophic relationship between wind and mass in a general form that properly accounts for the latitudinal variation of the Coriolis parameter. The balanced mass field in terms of geopotential height ϕ on the globe can be easily obtained by solving the Poisson equation with advection of the planetary vorticity as a source. However, the solutions for the rotational stream function, ψ , are not obvious because the Coriolis parameter vanishes at the equator, leading to singularities. Earlier

¹ To whom correspondence should be addressed: Global Hydrology and Climate Center, 320 Sparkman Drive, Huntsville, Alabama 35805. Fax: (256)-961-7788. E-mail: hi.lu@msfc.nasa.gov.

studies on the spectral LBE for ψ by Eliassen and Machenhauer [1], Merilees [2], Baer [3], Wiin-Nielsen [4], and Daley [5, 6] showed various degrees of singularity effects in either the spectral domain or physical space.

In the early evolution of numerical weather prediction, the linear balance equation assumed penultimate status (next to the nonlinear balanced model) in the hierarchy of the filtered models (e.g., Haltiner and Williams [7]). Difficulties in ensuring a balance condition and obtaining a nonsingular balanced wind field in the tropics may have contributed to its losing popularity since the 1970s. However, a geostrophic height-wind relationship is still incorporated in the state-of-the-art data assimilation systems during the increment analysis procedure (e.g., Schubert *et al.* [8] and Kalnay *et al.* [9]). Since a final analysis is made up of an analyzed increment and a first-guess field obtained from a previous integration of a general circulation model, one can at most expect a quasi-linear balance condition to exist in the assimilated data. It would be diagnostically useful to retrieve the balanced wind from the reanalysis data if such a condition exists.

Similar numerical difficulties arise when divergent winds are retrieved on the basis of the vorticity budget equation, known as the χ problem (Sardeshmukh and Hoskins [10]). The balance χ equation (see Eq. (5) of [10]) is formally identical to the linear balance ψ equation, provided that all the higher order terms are treated as known variables. Like the LBE, the difficulties in solving a χ problem lie in how to circumvent the tropical singularities, assuming that a balance in the vorticity budget exists. Sardeshmukh and Hoskins [10] argued that their numerical method does not “see the equator very clearly, hence there is no difficulty in obtaining the solution even slightly off the equator.” In reality, the solutions so obtained, e.g., Sardeshmukh [11] and Sardeshmukh and Liebmann [12], resulted in a relatively large residual in the vorticity budget calculations near the equator. No explanation was given as to the source and implication of this residual. Mo and Rasmusson [13] also noted that the solution near the equator is particularly sensitive to errors in the source function. If using the solution of the χ problem to estimate the diabatic heating in the tropics (Newman *et al.* [14]) is to provide meaningful information, a reliable numerical scheme must first be developed and its numerical properties understood.

The purpose of this paper is to document a potentially powerful inverse technique that we have developed to retrieve the two types of balanced winds mentioned above. The prototype of the technique is applied directly to retrieve the balanced rotational winds (or vorticity). The technique is then employed to retrieve the balanced divergent winds (or divergence) in a functionally iterative manner.

In deriving the spectral LBE, one must deal with the issue that the determinacy of the equation system depends upon how the spectral coefficients are truncated. All the previous works have been based upon certain types of truncations. For example, a fully determined system was constructed by assuming equal numbers of symmetric and antisymmetric modes. An overdetermined system was constructed (Baer [3]) by assuming that ψ is represented by the antisymmetric modes and ϕ is represented by the symmetric modes with one mode more than ψ . In the inverse technique to be described, we will construct an underdetermined system with proper truncations at the end modes. We have developed a unified methodology suitable for all types of truncations, thereby not only recovering the classical results but also demonstrating a systematic way of improving the retrievals.

In Section 2, the mathematical background for the present study will be reviewed with emphasis placed on the interrelation between the least-squares systems that are to be inverted, and their original spectral equation systems which can be either fully determined

(FD), underdetermined (UD), or overdetermined (OD). These three types of linear systems will be solved as a generalized inverse problem.

In Section 3 we will present results from actual calculations using the data produced by the NCEP/NCAR reanalysis project (Kalnay *et al.* [9]). In particular, we will compare results from different types of truncations, showing the effects of tropical singularities on the retrieved ψ field. We will also present examples of the divergence retrievals using the same data source.

In Section 4, several issues concerning the tropical singularity and the numerical properties of our present method and Sardeshmukh–Liebmann’s scheme will be discussed. We conclude that both balance equations are better treated as an inverse problem if physically meaningful retrievals are to be obtained.

2. THEORETICAL BACKGROUND

2.1. The Spectral LBE and Its Kernel Systems

Let the linear balance equation be written as

$$\nabla \cdot \mu \nabla \psi = \nabla^2 \phi = q \quad (1)$$

or

$$\mu \nabla^2 \psi + (1 - \mu^2) \partial \psi / \partial \mu = \nabla^2 \phi = q, \quad (2)$$

where ϕ is the geopotential height and ψ the stream function, which is related to the vertical component of the vorticity

$$\zeta = \nabla^2 \psi. \quad (3)$$

Both dependent variables are nondimensionalized by the earth’s radius, r_E , rate of rotation, and gravity. We use surface spherical coordinates λ and φ for longitude and latitude, respectively, and $\mu = \sin \varphi$. Notice that the right-hand side of Eq. (1) or Eq. (2) is denoted by a simple scalar function q which, in sigma coordinates, consists of a surface pressure term.

Upon expanding the dependent variables in a series of spherical harmonic functions, $P_{m+j}^m \exp(im\lambda)$, and utilizing the recursion relationships for the associated Legendre polynomials, we obtain the following spectral LBE which is equivalent to that of Eliassen and Machenhauer [1]

$$b_{j-1} \zeta_{j-1} + a_{j+1} \zeta_{j+1} = q_j, \quad (4)$$

$$\zeta_j = -c_j \psi_j, \quad (5)$$

where

$$a_j = a_{m+j}^m = (m+j+1)(m+j-1) \varepsilon_{m+j}^m / c_j, \quad (6)$$

$$b_j = b_{m+j}^m = (m+j)(m+j+2) \varepsilon_{m+j+1}^m / c_j, \quad (7)$$

$$c_j = c_{m+j}^m = (m+j)(m+j+1) / r_E^2, \quad (8)$$

with $\varepsilon_{m+j}^m = [(m+j)^2 - m^2]^{1/2}[4(m+j)^2 - 1]^{-1/2}$. Here, m denotes the longitudinal wave number and $m+j$ denotes the order of the Legendre polynomial (or the ordinal wave number).

The coefficient matrices associated with the linear system (4) for any m are hereafter called the “kernel” matrices of the spectral LBE and are denoted by K . Let the spectral coefficients be partitioned into symmetric (even) and antisymmetric (odd) components: $\vec{\zeta}_s = (\zeta_0, \zeta_2, \zeta_4, \dots)$, $\vec{\zeta}_a = (\zeta_1, \zeta_3, \zeta_5, \dots)$, etc. As indicated in (4), there is a parity relationship between ζ (or ψ) and q (or ϕ); namely, $\vec{\zeta}_s$ and $\vec{\zeta}_a$ are determined by \vec{q}_a and \vec{q}_s , respectively. Thus for each m the spectral LBE is solved by two independent kernel systems: $K_s \vec{\zeta}_s = \vec{q}_a$ and $K_a \vec{\zeta}_a = \vec{q}_s$. Depending upon truncations, the kernel matrix systems may be fully determined, overdetermined, or underdetermined.

2.2. Least-Squares Formulations

The standard procedure for obtaining the least-squares solution of a given kernel system, $K \vec{\zeta} = \vec{q}$, is to solve the corresponding normal equation

$$K^T K \vec{\zeta} = K^T \vec{q}, \quad (9)$$

where K^T is the transpose of K .

Upon multiplying the j th equation in (9) by c_j for all j , we obtain the scale-weighted normal equations as

$$\hat{K}^T K \vec{\zeta} = \hat{K}^T \vec{q}, \quad (10)$$

where $\hat{K}^T = KC$, $C = [c_j \delta_{i,j}]$ is a diagonal matrix and δ_{ij} is the Kronecker delta.

One can arbitrarily transform the normal equation by multiplying the individual equations in the equation system by an arbitrary power of c_j . The solutions will be identical when the kernel is either FD or OD. In the UD cases, however, the solutions are generally different. We will show that the results of retrieving rotational winds from (10) are more realistic than from (9), presumably due to its scale selectivity.

The least-squares formulations can be alternatively derived based upon a variational analysis of the equation residual. As described in Appendix A, the most crucial step of the derivation occurs when the dependent variables are expressed in a truncated series, which varies with the type of truncation chosen.

2.3. Fully Determined Systems

To obtain a FD system for the nonzonal ($m \neq 0$, called “eddy” in meteorology) ζ_a and ζ_s as in Daley [5], the truncation limit J must be an odd number; i.e., the numbers of symmetric and antisymmetric modes are equal, hereafter called even truncation (ET). It is easy to show that in the two kernel systems $K_s \vec{\zeta}_s = \vec{q}_a$ and $K_a \vec{\zeta}_a = \vec{q}_s$, K_s is an upper bidiagonal matrix, while K_a is a lower bidiagonal matrix. Hence the solution for ζ_s can be obtained by backward substitution and for ζ_a by forward substitution. Note that in the course of direct substitution (called the recurrence method in the literature), the end-mode conditions $\zeta_{-1} = \zeta_{J+1} = 0$ are assumed.

In the case of $m = 0$, however, the truncation must be ended with an additional symmetric mode, hence called odd truncation (OT), in order for the systems to be FD,

because $a_1 = b_0 = q_0 = \psi_0 = \zeta_0 = 0$. It is easy to show that the kernel matrices for the symmetric/antisymmetric zonal components are lower/upper bidiagonal; hence the forward/backward substitution shall be taken to solve the systems, assuming the starting values $\zeta_0 = 0$ and $\zeta_{2N+1} = 0$, respectively. However, the end result of ζ_1 (or ψ_1) from the backward substitution is exactly equal to the product of mean geostrophic angular momentum and a known constant. This is why Eliassen and Machenhauer [1] used an estimate of mean geostrophic angular momentum as the starting value of ζ_1 for the forward substitution.

In the above analyses, the end-mode conditions $\zeta_{J+1} = \zeta_{2N+1} = 0$ are assumed for the backward substitution, but no assumptions are needed for the higher even modes, e.g., ζ_{J+2} and ζ_{J+4} . However, those higher even modes can be resolved by extending the forward substitution beyond the “source range,” i.e., where $q_j = 0$. This results in an “energy spill” into the “inertial range,” a phenomenon known as “non-terminating energy spectrum” in Merilees [2] and Baer [3], which better depicts the singular behavior (in analogy to a delta function versus a white spectrum) at the equator.

We will only use the forward/backward substitution to interpret the numerical properties associated with the FD systems. It is clear that all the direct methods, including the ones used by Daley [5], are equivalent when the kernel matrix is fully determined.

2.4. Overdetermined Systems

When the truncation is odd, the kernel systems for the nonzonal $\vec{\zeta}_a$ are overdetermined if the end-mode conditions, $\zeta_{-1} = \zeta_{J+1} = 0$, are assumed. Thus $K_a \vec{\zeta}_a = \vec{q}_s$ is

$$\begin{pmatrix} a_1 & . & . & . \\ b_1 & a_3 & . & . \\ . & b_3 & a_5 & . \\ . & . & b_5 & a_{2N-1} \\ . & . & . & b_{2N-1} \end{pmatrix} \begin{pmatrix} \zeta_1 \\ \zeta_3 \\ \zeta_5 \\ \zeta_{2N-1} \end{pmatrix} = \begin{pmatrix} q_0 \\ q_2 \\ q_4 \\ q_6 \\ q_{2N} \end{pmatrix}. \quad (11)$$

Similarly, when the even truncation is used to solve for the zonal ($m = 0$) ζ_s , the resulting kernel systems are overdetermined.

The end-mode conditions assumed in the OD systems ensure no energy spill into the inertial range as occurred in the FD systems. However, in order to satisfy simultaneously the two end conditions, $\zeta_{-1} = \zeta_{J+1} = 0$, the spectral LBE can only be approximated in least squares. This is analogous to the kinematic adjustment of the vertical velocity profile using the continuity equation (O’Brien [15]) when both the upper and lower boundary conditions are constrained.

Following the procedure described in Section 2.2, the resulting least-squares OD system for the nonzonal ζ_a is

$$K_a^T K_a \vec{\zeta}_a = K_a^T \vec{q}_s, \quad (12)$$

or

$$a_j b_{j-2} \zeta_{j-2} + (a_j^2 + b_j^2) \zeta_j + a_{j+2} b_j \zeta_{j+2} = (a_j q_{j-1} + b_j q_{j+1}), \quad (13)$$

where $j = 1, 3, \dots, 2N - 1$, and $\zeta_{2N+1} = 0$.

Note that the last diagonal element of $K_a^T K_a$ can be approximated by $2a_j^2$ when $J = 2N - 1$ is large, while it equals to a_j^2 in a least-squares FD system. Therefore, the smallest

eigenvalue for the OD system is considerably larger than the FD counterpart and it is expected that the response to tropical singularities by the OD systems will be weaker than that by the FD systems.

2.5. Underdetermined Systems

When the truncation is odd, the kernel systems for the nonzonal ζ_s are obtained by dropping the last equation of a fully determined system $K_s \vec{\zeta}_s = \vec{q}_a$; i.e.,

$$\begin{pmatrix} b_0 & a_2 & \cdot & \cdot \\ \cdot & b_2 & a_4 & \cdot \\ \cdot & \cdot & b_{2N-2} & a_{2N} \end{pmatrix} \begin{pmatrix} \zeta_0 \\ \zeta_2 \\ \zeta_4 \\ \zeta_{2N} \end{pmatrix} = \begin{pmatrix} q_1 \\ q_3 \\ q_{2N-1} \end{pmatrix}. \quad (14)$$

Similarly, one obtains an UD kernel system for the zonal ζ_a in an even truncation. The above described two UD systems are mandatory due to the chosen truncations. However, other UD systems can be formulated if deemed useful.

We consider an UD system for solving the nonzonal ζ_a . It results from dropping the first equation from a fully determined system $K_a \vec{\zeta}_a = \vec{q}_s$; i.e.,

$$\begin{pmatrix} b_1 & a_3 & \cdot & \cdot \\ \cdot & b_3 & a_5 & \cdot \\ \cdot & \cdot & b_{J-2} & a_J \end{pmatrix} \begin{pmatrix} \zeta_1 \\ \zeta_3 \\ \zeta_5 \\ \zeta_J \end{pmatrix} = \begin{pmatrix} q_2 \\ q_4 \\ q_{J-1} \end{pmatrix}, \text{ for } m \neq 0. \quad (15)$$

Essentially, UD systems arise from the consideration that the spectral LBE excludes the two end-mode conditions usually assumed in either a FD or an OD system.

The standard procedure for solving an UD system is based upon the least-squares approximations discussed in Section 2.2. However, it is important to note that the least-squares UD system is ill posed as one of the eigenvalues in the matrix system is zero. Therefore the solutions will not be unique.

2.6. Minimum-Length Solutions (MLS)

Two of the most frequently used inverse techniques for solving a least-squares UD system are constrained linear inversion (CLI) and singular value decomposition (SVD). They attain a solution by either suppressing or omitting the presence of the singular eigenmodes that exist in a least-squares system.

The CLI (see Appendix A) includes a diffusion term in a least-squares system as a stabilizing factor; i.e., $(K^T K + \gamma I) \vec{\zeta} = K^T \vec{q}$, where I is the identity matrix. Note that the eigenvectors of $K^T K + \gamma I$ are those of $K^T K$ but the eigenvalues are each incremented by γ . When a small γ is included the singular eigenvalues are greatly increased (relatively speaking) thereby reducing the singular calculations, but the others are not greatly altered, leaving the main part of the solutions relatively unchanged. Twomey [16] described a post-facto method for selecting the γ factor when the numerical method for solving a linear system does not require calculations of eigenvalues.

The procedure of SVD generally requires calculations of eigenvalues. However, when the linear systems are ‘‘inverted’’ all the reciprocals of zero eigenvalues are set to zero resulting in a minimum-length solution (e.g., Noble and Daniel [17]). In fact, we have verified that

the solutions from the SVD are practically identical with those from the CLI when γ is appropriately chosen. Tribbia and Madden [18] applied the SVD technique to solve the Fourier transformed LBE in computing stationary Rossby wave amplitudes.

The justification for taking a MLS is usually based upon the notion that singular eigenmodes are the cause of computational instability and, hence, must be completely suppressed. In reality, the contributions from singular eigenmodes are arbitrary. Whether a MLS is desirable would depend on the nature of the problem and how the least-squares system is formulated. We will show later that a realistic retrieval of vorticity is attainable from the MLS of a scale-weighted normal equation (10). However, we have not succeeded in obtaining a realistic retrieval of divergence by taking the MLS of a similarly derived least-squares problem.

2.7. Similarity Transformation

Let either one of the proposed least-squares systems (9) or (10) for each m be denoted as $A\vec{x} = \vec{y}$. Suppose that the eigenvalues of A are $(\lambda_0, \lambda_1, \lambda_2, \dots, \lambda_J)$ and the corresponding set of eigenvectors $(\vec{e}_0, \vec{e}_1, \dots, \vec{e}_J)$ are stored columnwise in the modal matrix E . Then $E^{-1}AE = [\lambda_i \delta_{ij}]$, where δ_{ij} is the Kronecker delta, and E^{-1} is the inverse of E . The similarity transformation method (e.g., Hildebrand [19]) inverts the least-squares system as

$$\vec{x} = E \{ [\lambda_i^{-1} \delta_{ij}] E^{-1} \vec{y} \}. \quad (16)$$

Basically, the procedure of inversion consists of a linear combination of the eigenmodes with the coefficients determined by the projections of the source function weighted by the reciprocals of the corresponding eigenvalues. We used Linear Algebra Package (e-mail lapak@cs.utk.edu for more information) for the required calculations of the eigenvalues and eigenvectors (both left and right).

Note that each eigenfunction has as many zeros as the assumed truncation limit $J + m$. As the eigenvalue increases the locations of the highest peaks shift progressively toward the poles. When the kernel is UD the smallest eigenvalue λ_0 is zero and the corresponding eigenvector \vec{e}_0 is peaked at (when even) or near (when odd) the equator.

The inverse formula defined in (16) can be carried out freely when the kernel system is either FD or OD. When the kernel system is UD the formula is invalid because one of the eigenvalues for each m is zero. Surprisingly, the projections of the source function, in terms of \vec{y} , on the singular eigenmodes are also found to be zero within the same computational tolerance of obtaining the zero eigenvalues; hence the results are undefined. We shall carefully implement the similarity transformation method when solving for a least-squares UD system so that the nonunique nature of the problem is retained.

2.8. Generalized (Pseudo) Inverses

With all the generalities included, the inverse of the spectral linear balance equation can be formulated as

$$\vec{\zeta} = \sum_{j=1}^J s_j \vec{e}_j + s_0 \vec{e}_0. \quad (17)$$

The first term in (17) contains the so-called principal components, and the second term is called the singular component. The coefficients s_j associated with the principal components are computed as the projections of the source vector $\hat{K}^T \vec{q}$ on \vec{e}_j in accordance to the formula (16). The coefficient s_0 associated with the singular eigenvector \vec{e}_0 is zero if the kernel is either FD or OD, and undefined when the kernel is UD.

When the kernel is UD, s_0 must be determined on the basis of other constraints. For example, s_0 is zero if the retrievals are constrained to have a minimum length. When an independent set of measurements or estimates of the retrieving variable are available, the standard approach of incorporating this information is to formulate a bias constraint (e.g., O'Brien [15], Twomey [16]) in a variational analysis that minimizes the *data misfit*, or *relative length*, of the retrieving variable.

We employ the bias constrained linear inversion method in such a way that we minimize the square difference between the retrievals and independent measurements *solely* on the singular components. It is easy to show that the minimum occurs at

$$s_0 = \langle \vec{\zeta}^*, \vec{e}_0 \rangle, \quad (18)$$

i.e., as the projection of the independent measurement $\vec{\zeta}^*$ on the singular eigenvector for each m . Note that including a nonzero singular component will not change the residual of the kernel system. However, it may result in a pseudo-residual (discussed later) and an increase in the retrieval's variance which is bounded by the independent measurement.

Here, we take $\vec{\zeta}^*$ from the NCEP/NCAR reanalysis for the vorticity retrievals. In the case of divergence retrievals described next the reanalysis divergence $\vec{\delta}^*$ would replace $\vec{\zeta}^*$ in computing the singular components. The chosen data are well suited to illustrate how the present inverse method works particularly when comparing the results from different truncations and numerical schemes.

2.9. Application for the Divergence Retrievals

The aforementioned inverse method for vorticity retrievals can be applied to retrieving a divergence based upon the χ problem in a functional iterative manner

$$\nabla \cdot \mu \nabla \chi^{(n+1)} = q^{(n)} = B - \nabla \cdot \zeta \nabla \chi^{(n)}, \quad (19)$$

where B stands for the sum of all tendency terms in the vorticity budget equation, and (n) denotes the iteration steps. Analogous to (3), the velocity potential χ is related to the divergence δ by $\nabla^2 \chi = \delta$.

The convergence rate of the iterations, $|\delta^{(n+1)} - \delta^{(n)}|^2 / |\delta^{(n)}|^2$, varies with the chosen resolution and type of truncation that affect the tropical singularities and with the quality of data taken to compute the singular components. For a medium resolution model using an UD kernel to approximate (19), taking the NCEP reanalysis data to compute the singular components, it takes less than 30 iterations to achieve an asymptotic convergence rate of 10^{-10} .

2.10. Sardeshmukh–Liebmann's Scheme

Sardeshmukh and Liebmann [12] developed an iterative scheme, hereafter referred to as SL93, for solving a χ problem. The scheme is adapted here to solve the LBE in terms of

the vorticity coefficients

$$\zeta^{(n+1)} = \zeta^{(n)} + 2\alpha\nabla^{-2}\{\nabla \cdot \mu\nabla\varepsilon R^{(n)}\}, \quad (20)$$

where R is the residual of the LBE, (n) is the iteration index, α is the iteration step, and ε is a latitudinal weight function, $1/(\mu^2 + \mu_0^2)$. In our implementation of the method, $\alpha = 0.4$ and $\mu_0 = 0.6$ were chosen, and the initial vorticity field was set to zero everywhere. When $\zeta^{(n)}$ and $R^{(n)}$ are properly truncated in each iteration, the scheme will perform equivalently to solve the three types of kernel systems, except for solving ζ_a in an UD system (15). There is no proper way of including the first symmetric modes of $R^{(n)}$ in such a case.

The iterative scheme may suffer from poor convergence when the kernel system is FD. We found that the convergence rate, which is measured in terms of $|\zeta^{(n+1)} - \zeta^{(n)}|^2/|\zeta^{(n)}|^2$, generally reaches 10^{-4} within 300 iterations. However, to obtain a converged ζ_a solution that can be judged as numerically equal to the one obtained from the direct FD solver, it required more than 4800 iterations at triangular truncation T16. These converged solutions are substantially different from the quasi-converged solutions obtained within 300 iterations.

The numerically “exact” solutions can be obtained only when the kernel equations are of either FD or UD type. The converged solution for an OD system generally results in a nonzero residual. Furthermore, the converged solution for an UD system shall be viewed as one of the infinitely many solutions that is attainable by the numerical scheme.

3. RESULTS

3.1. Calculations with the NCEP/NCAR Reanalysis Data

Calculations for the balanced winds were made with the reanalysis data obtained from the NCEP/NCAR 40-year reanalysis project (Kalnay *et al.* [9]).

The reanalysis data (T62, 28 sigma levels) for September 1987 were taken to compute the LBE and the vorticity budget equation in the sigma coordinates using the spectral transform method (Machenhauer [20]) and the results, along with the wind data, were filtered to the desired truncations. In the present study, we retrieve vorticity fields on sigma = 0.251 for 00Z September 1 and divergence fields on sigma = 0.1326 for the monthly mean. Only the nonzonal components of the retrievals are discussed here, although a full spectrum is needed to compute the divergence retrievals.

In the conventional triangular truncation, the number of ordinal modes alternates between even and odd as the longitudinal wave number (m) increases. For the purpose of illustrating the present numerical methods, we designate four truncation systems such that the last modes for each m are all either symmetric (as odd truncation, namely, OT32 and OT16) or antisymmetric (as even truncation, namely, ET32 and ET16). We also denote the inverse methods as FD, OD, and UD retrievers, respectively, in accordance with the determinacy of the kernel systems. Two retrievers using the least-squares UD systems (9) and (10), denoted by UD1 and UD2, respectively, were tested. The UD retrievers that include singular components are designated as UD1 and UD2. For a given truncation, a complete global retrieval of vorticity is made from a collection of ζ_s/ζ_a retrievals by one of the following combinatory retrievers: FD/FD, UD1/OD, UD1/UD1, UD2/UD2, etc. The above notations are adapted for the divergence retrievals, despite the fact that the contributions of δ_s and δ_a are combined before updating the corrector in each iteration (19).

From the retrieved vorticity or divergence coefficients, the corresponding wind fields were computed using the same assumed spectral truncations. The longitudinal RMS differences between the retrieval and reanalysis wind vectors, called *wind misfits*, were then evaluated. In addition, the advective terms were recalculated which yielded the *equation residuals* or sometimes called *dynamics misfits*. It will become evident later that wind misfits to a great extent measure the responses of tropical singularities, while dynamics misfits manifest the over- or underdeterminacy in the system.

3.2. Retrievals for Vorticity

Figure 1 shows the degrees of imbalance associated with the LBE in OT16, in RMS differences of the two sides of the equation. It reveals that the relative imbalance is generally less than 20% in the middle and high latitudes and less than 40% in the tropics. Here the imbalance is due in part to the “model error” of using the LBE as a diagnostic model and in part to the “measurement errors” from all sources. Figure 1 also shows that a large difference between the ET16 and OT16 analyses on the RHS exists due to the offsets between the two truncation limits. This suggests that the retrievals based upon T16 may be sensitive to the imposed end-mode conditions; i.e., $\zeta_{J+1} = 0$. In addition, the RMS equation residuals (denoted by “res”) resulting from the UD2/UD2 and UD1/OD retrievers are included in Fig. 1, which will be discussed shortly.

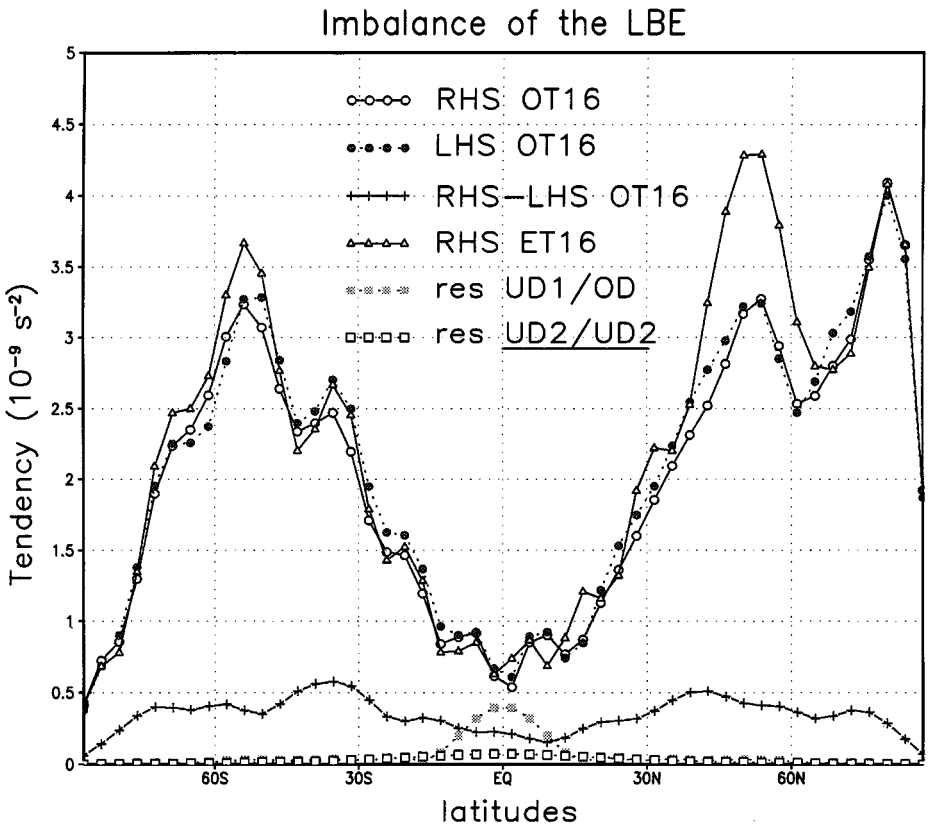


FIG. 1. Imbalance calculations for the linear balance equation in OT16 and ET16 using the NCEP/NCAR reanalysis data. The two curves labeled as “res” are the residuals resulting from the UD1/OD and UD2/UD2 retrievers.

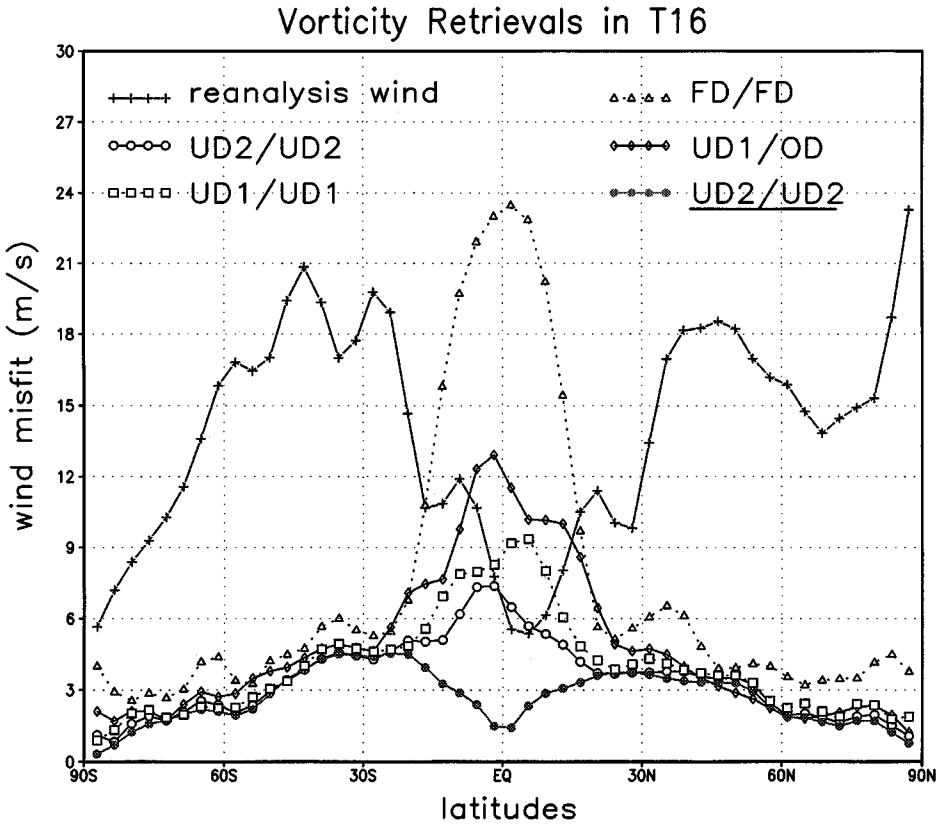


FIG. 2. Root-mean-squares of the reanalysis wind and wind misfits in OT16 and ET16 resulting from various combinatory retrievers for ζ_s/ζ_a .

Figure 2 shows the wind misfits resulting from various combinatory retrievers for ζ_s/ζ_a . Note that while the FD/FD retrievers are used for the ET16 runs, the rest are used for the OT16 runs. It reveals that in the middle and high latitudes, the relative wind misfits are comparable to the relative imbalance of the LBE mentioned previously. However, in the tropics there is a wide range of misfits resulting from different retrieving schemes. Not surprisingly, the greatest relative wind misfit, higher than 300%, was obtained in the FD/FD retrievals. This is caused by the exceedingly large retrieved wind speeds in response to tropical singularities.

We have run an experiment on the “energy spill” phenomenon (discussed in Section 2.3) by increasing the resolution for ζ_a to ET32, while holding the resolution for ϕ_s unchanged in ET16. Consistent with the finding of Daley [5, 6], the wind misfits by ζ_a increase, while the misfits by ζ_s are invariant with the enhanced resolutions.

The wind misfits resulting from the UD1/OD retrievers are nearly equal to those from the SL93 scheme; hence only one is shown. It can be demonstrated that the small differences between the two lie in the ζ_s components due to the fact that the solutions for the UD kernels attained by the SL93 scheme are not in a minimum length.

The singularity responses in the UD1/OD retrievals are moderate in comparison to the FD/FD retrievals. By omitting the singular mode contributions, the UD1/UD1 and UD2/UD2 retrievers considerably reduce the wind misfits. Including the singular

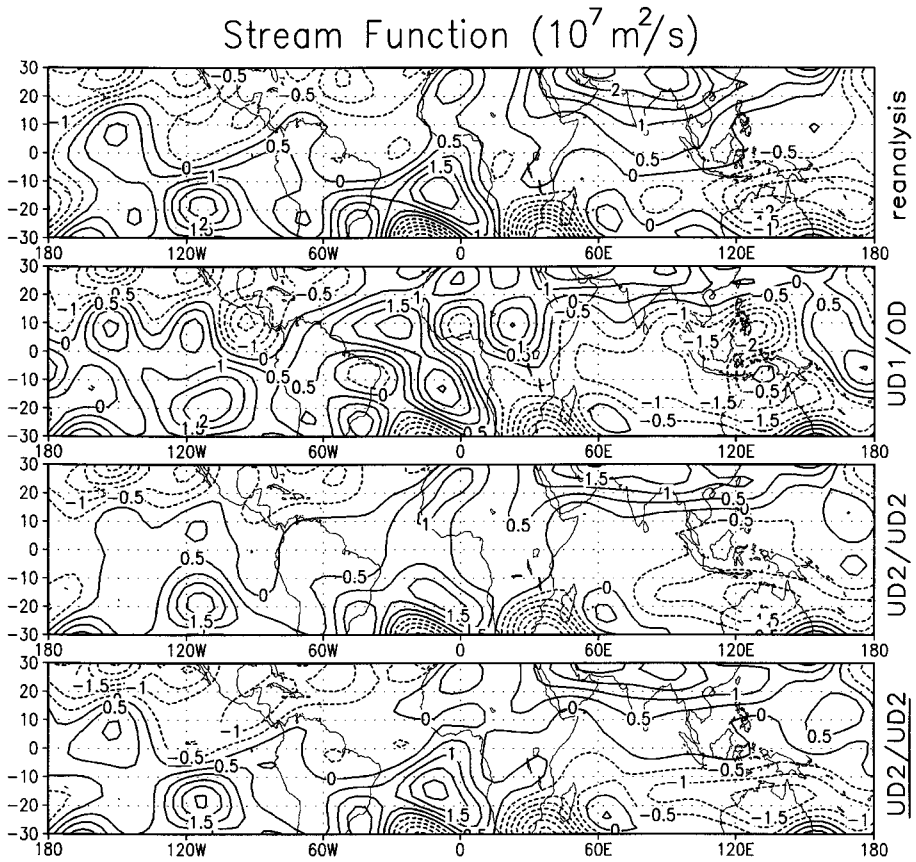


FIG. 3. Stream function fields in OT16 resulting from the NCEP/NCAR reanalysis and various combinatory retrievers for ζ_s/ζ_a .

components, the UD2/UD2 retrievers further reduce the relative wind misfit down to 30% in the tropics, which is in the same order of magnitude as the relative imbalance of the LBE discussed previously.

Figure 3 displays the two-dimensional ψ fields obtained from the reanalysis and various retrievals. It is seen that the UD1/OD retrievals consist of several spurious, intense synoptic features not present in the reanalysis. The strong dipoles along the equator between 0°W and 60°W are equivalent to the strong pairings of convergence and divergence in the solution of a χ problem described in Mo and Rasmusson [13]. This peculiar feature is induced by the end-mode conditions assumed in the OD retriever.

Omitting the singular mode contributions, the UD2/UD2 retrievers result in a relatively featureless ψ field, reminiscent of a linear interpolation across the equator. Adding the singular components, the UD2/UD2 retrievers bring about a closer resemblance to the reanalysis wind field. However, the geostrophic balance condition associated with the UD2/UD2 retrievals is actually degraded in some regions of the tropics, as discussed next.

3.3. Equation Residuals

The FD retrievals satisfy exactly the model equation; therefore no residual results. The residuals generally result in the OD retrievals because of the end-mode conditions involved.

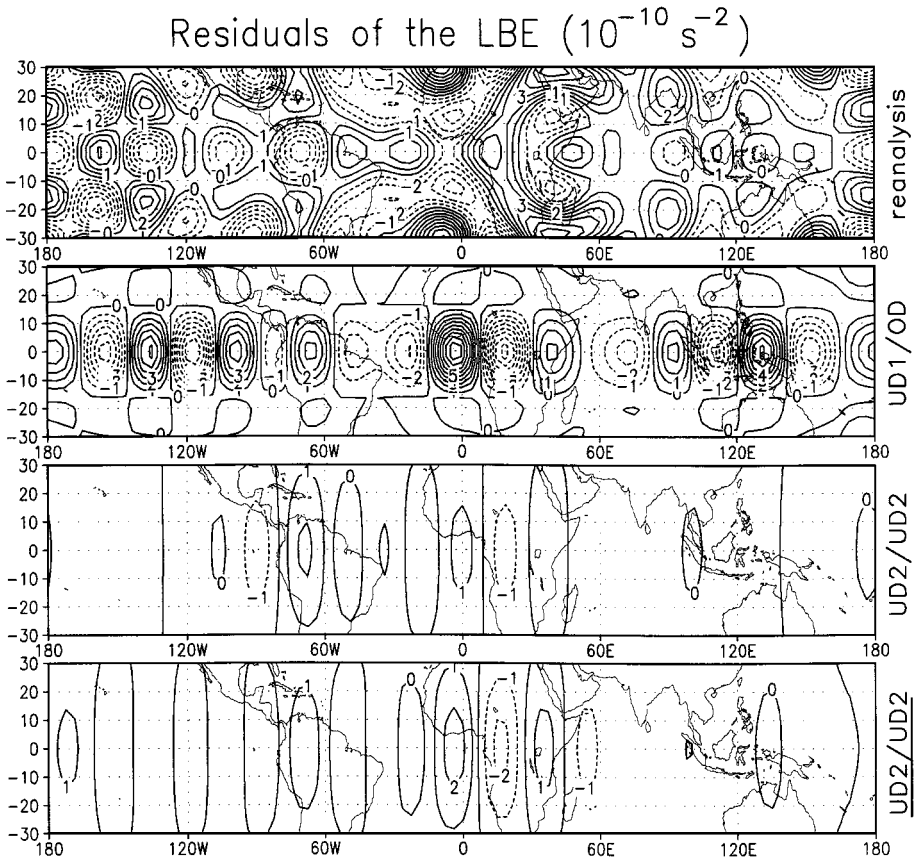


FIG. 4. Imbalances of the LBE in OT16 resulting from the NCEP/NCAR reanalysis and various combinatory retrievers for ζ_s/ζ_a .

The UD retrievals also satisfy exactly the corresponding kernels. However, a “pseudo residual” results when the residual calculations due to ζ_a include the first ordinal modes on q_s , which were excluded in the formulation of the kernel systems (15). There is no pseudo residual that results when using an UD retriever for ζ_s . We shall take pseudo residuals in the UD retrievals and regular residuals in other retrievals to compare how well the retrieved winds satisfy the balance condition.

Figure 4 compares the two-dimensional distributions of the residuals resulting from the OT16 runs. Here, only the symmetric components are displayed. Residuals are generally small in the high latitudes; hence they are not shown.

The residuals from the UD1/OD retrievers (due only to OD part) are characterized by a train of modulated small cells along the equator, with a latitudinal scale roughly in proportion to the truncated ordinal wavelength. In the present case, the magnitudes are generally larger than the observed imbalance of the equation within the $\pm 15^\circ$ latitude band (see also Fig. 1). The residuals from the iterative scheme (not shown) are nearly identical to the UD1/OD retrievers except for a slightly larger magnitude in the higher latitudes.

The pseudo residuals from the UD2/UD2 retrievers are characterized by a cluster of tropical cells near Africa and South America, with latitudinal length scales corresponding to the first ordinal wave numbers. The magnitudes are typically smaller than the observed

imbalance of the LBE (see also Fig. 1). When the singular components are added into the retrievals, the resulting pseudo residuals are reduced in some regions while increased in others. The high residual region between 20°W and 60°E may be attributed to a relatively poor balance condition existing in the mid-latitudes. It appears that including the reanalysis wind data does not improve the accuracy of the retrievals, in terms of the degree of geostrophy, beyond the limit inherent in the data.

3.4. Divergence Retrievals for a χ Problem

Figure 5 shows the degree of imbalance in the vorticity budget calculations based upon the reanalysis data. The LHS represents the absolute vorticity stretching term, while the RHS represents the sum of the rest of terms in the budget equation and is denoted as “source term” B in (19) for the present χ problem. The source term and stretching term are nearly equal in magnitude; both possess a minimum near the equator and peaks in the subtropics. However, the RMS differences of these two terms (i.e., imbalance) generally exceed 20% of the individual terms, except for the northern hemispheric subtropics. In the tropics, the imbalance exceeds 50%, which is worse than the imbalance of the LBE indicated in Fig. 1. The imbalance in the budget calculations may be attributed to the “systematic errors” (Kanamitsu and Saha [21]) in the forecast model used for the 4-D data

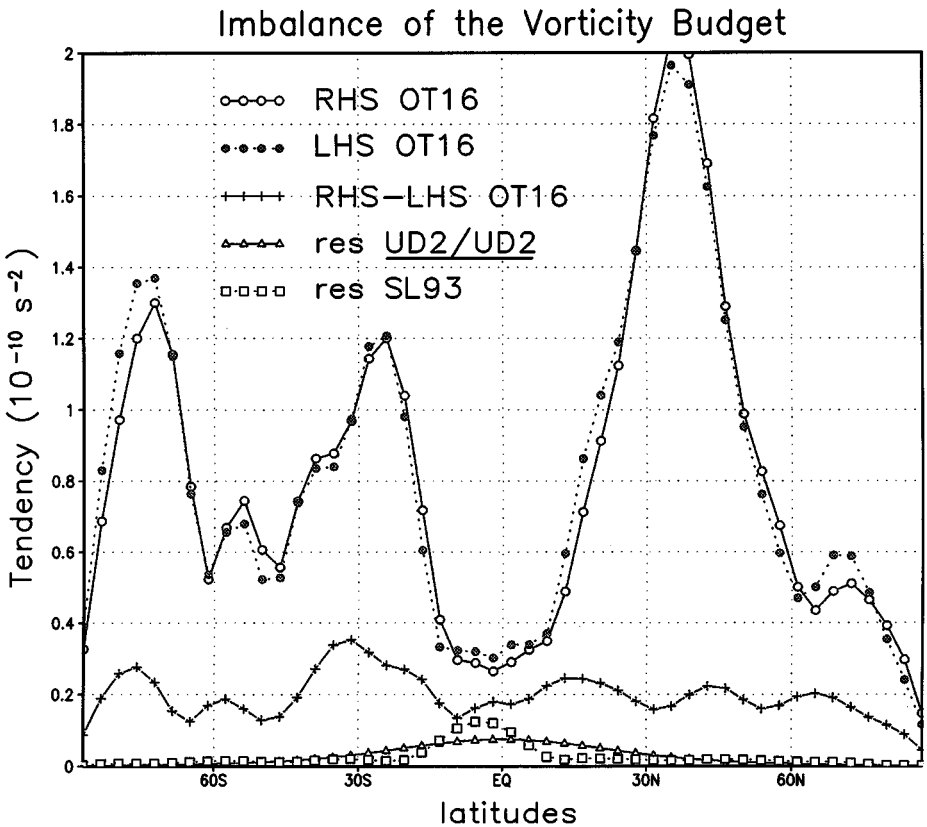


FIG. 5. Imbalance calculations for the vorticity budget equation in OT16 using the NCEP/NCAR reanalysis data. Two curves labeled as “res” are the residuals resulting from the UD2/UD2 retrievers and the SL93 scheme.

Divergence Retrievals in T16

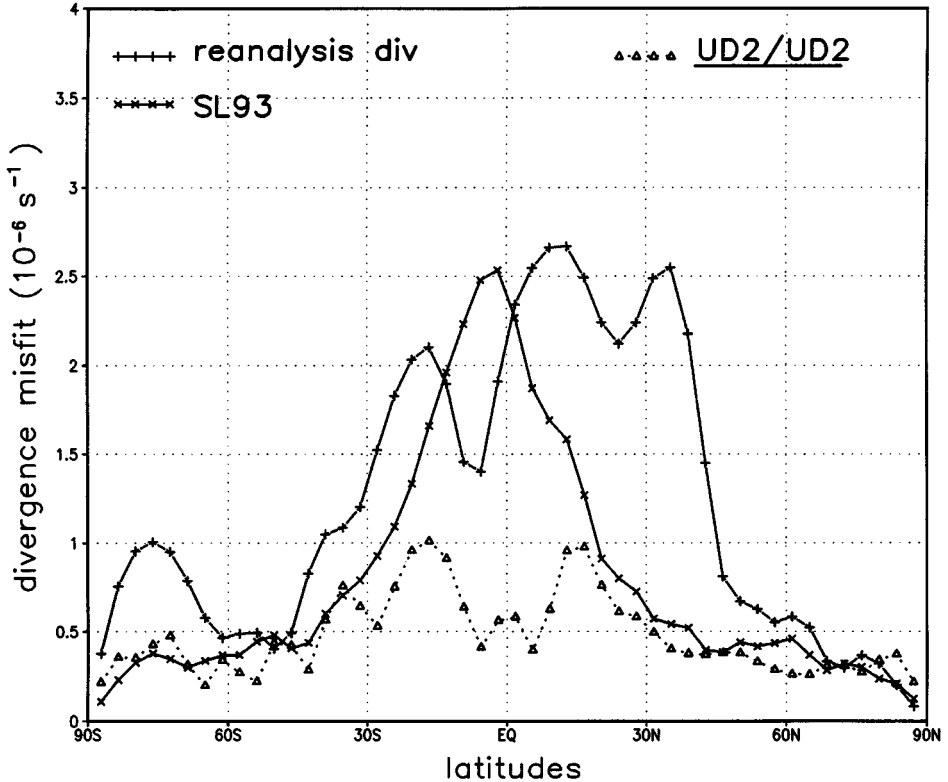


FIG. 6. Root-mean-squares of the reanalysis divergence and divergence misfits in OT16 resulting from the UD2/UD2 retrievers and the SL93 scheme.

assimilation, in addition to the differences arising from the ways of computing the individual tendency terms. However, owing to the monthly averaging that cancels the small scales and transient disturbances there is no evident offset between the OT16 and ET16 analyses (not shown). This implies that the divergence retrievals will be less sensitive to the end-mode conditions than the vorticity retrievals shown previously. Figure 5 also shows the RMS equation residuals resulting from the UD2/UD2 retrievers and the SL93 scheme, which will be discussed shortly.

In contrast to the LBE, the reanalysis divergences are relatively strong in the tropics (Fig. 6) in spite of a minimal vorticity tendency occurring there. We present only two divergence misfits (computed in the same way as wind misfits) obtained from the UD2/UD2 retrievers and the SL93 scheme. All the other retrievers mentioned in the previous section result in a misfit too large to be desirable. Clearly, the UD2/UD2 retrievers outperform the SL93 scheme in reducing the relative divergence misfits in the $\pm 20^\circ$ latitude band to a level that is comparable to the relative imbalance in the vorticity budget shown in Fig. 5. Near the poles, however, both methods give rise to a high divergence misfit relative to the reanalyses.

Figure 7 displays the divergence fields obtained from the reanalysis and retrievals in OT16. As expected, the UD2/UD2 retrievals show a fair resemblance with the reanalysis divergences, including the ITCZ in the Indian and western Pacific oceans. The SL93 scheme results in several spurious, intense synoptic features not present in the reanalysis.

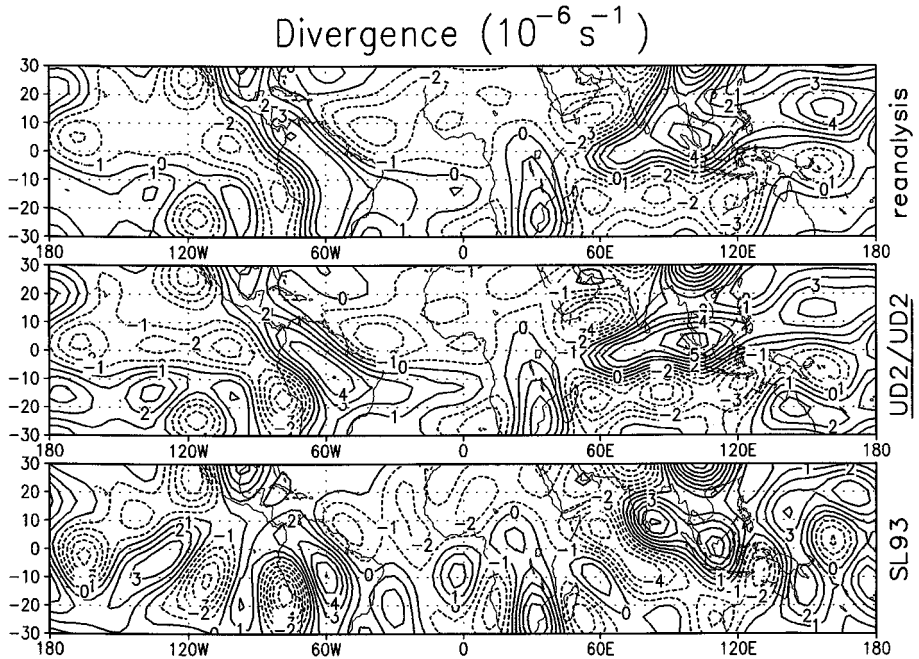


FIG. 7. Divergence fields in OT16 resulting from the NCEP/NCAR reanalysis, the UD2/UD2 retrievers, and the SL93 scheme.

The resulting residuals (Fig. 8) share the same characteristics as in the ψ retrievals. The pseudo residuals resulting from the UD2/UD2 retrievers are spread over the subtropics, while the residuals from the SL93 scheme are confined near the equator. The locations in which large residuals occur are considerably different between these two retrieving schemes, except in the western Pacific. As shown in Fig. 5, the two RMS residuals are both smaller than the relative imbalance of the vorticity equation.

4. DISCUSSION

4.1. The Existence of Tropical Singularities

The linear balance equation inherits the tropical singularities from the geostrophic equations in which the singularities associated with the antisymmetric parts of u and v cannot be removed unless corrections are made to the nonzonal ϕ_s and to the north–south gradient of the total ϕ_a , respectively. The observed ϕ fields generally do not satisfy the singularity removal conditions; hence the linearly balanced wind is theoretically infinite at the equator. In this paper, we have examined the responses of tropical singularities as a function of spectral truncations.

Observations and assimilated data are subject to errors and the balance equations are merely an approximation. To make use of the balance equations for diagnostic purposes we shall treat the equations as an inverse model, assuming that the singularities are removable by allowing a minimal adjustment to the source functions. In the case of LBE, we are retrieving the *components* of rotational winds that are geostrophically *best fit* with the mass field. In the case of the χ problem, we are retrieving the *components* of divergent winds that are

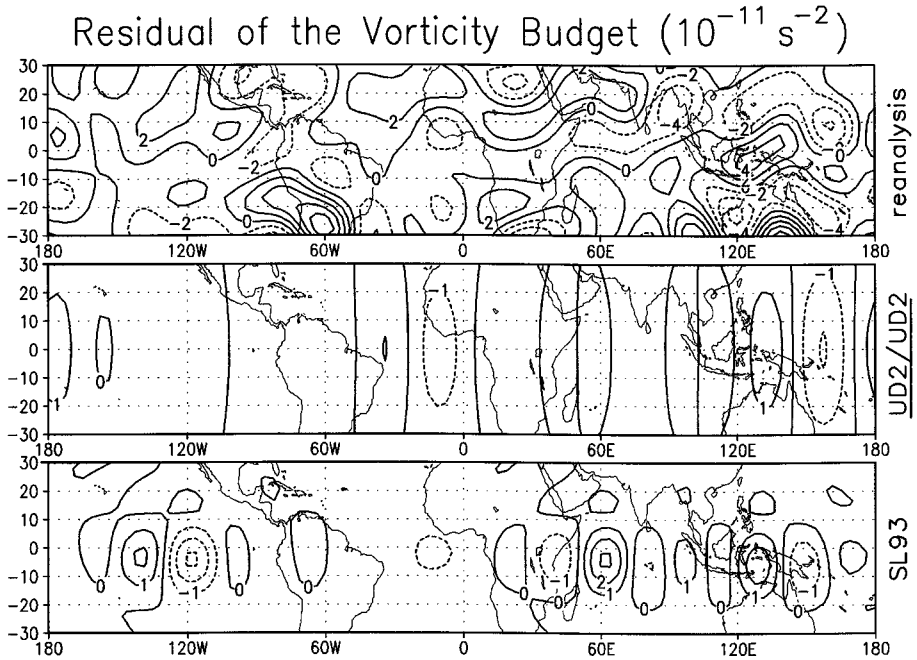


FIG. 8. Imbalances of the vorticity budget equation in OT16 resulting from the NCEP/NCAR reanalysis, the UD2/UD2 retrievers, and the SL93 scheme.

quasi-geostrophically *best fit* with the vorticity tendencies. At the same time, the retrievals are constrained to be least singular and to deviate minimally from the observational data at hand.

4.2. Singularity Responses as a Function of Truncations

Formulating the spectral LBE in a FD system is undoubtedly the most authentic way of demonstrating the existence of tropical singularities. The effects of tropical singularities are manifested in the energy spill phenomenon. The FD retrievals are exact and no dynamic misfit results, but the information obtained is useless in practice.

The OD retrievers reduce the singularity responses, but generally result in a nonzero residual. Depending upon the resolution that would affect the validity of the end-mode conditions, the resulting residuals may be large in comparison with the preestimated imbalance of the LBE.

The UD retrievers yield balanced rotational winds that are less singular and more realistic than those yielded by the FD and OD retrievers. Two possible explanations come to mind as to why the UD retrievals seem to be most desirable. First, the UD retrievers do not assume the end-mode conditions as the other two retrievers do, an attribute which is clearly not acceptable in the present T16 model. Second, the UD retrievers allow a partition of principal and singular components for better controlling the responses of singularities.

When the singular components are prescribed on the basis of the reanalysis winds which pose no singularity, the retrieved winds in the tropics conform more with the observation as expected. However, including the singular components does not improve the accuracy of the retrievals in terms of the required balance condition beyond the limit inherent in the reanalysis winds.

4.3. *Properties of the SL93 Scheme*

The fact that the vorticity retrievals from the SL93 scheme are identical to the FD/FD retrievers in the ET runs, while nearly identical with the UD1/OD retrievers in the OT runs, allows one to interpret the numerical properties associated with the SL93 scheme.

First, equation residuals are a byproduct of least-squares approximations when solving an OD system. They are independent of how the equation system is solved. The residuals shown in Sardeshmukh and Liebmann [12] are primarily a result of using the conventional triangular truncations in which one quarter of the linear systems are of OD type due to odd truncations. However, before the iterations are fully converged, a portion of residuals might originate from another quarter of the linear systems (for ζ_a and δ_a) which are of FD type due to even truncations.

Second, any numerical method of solving an UD system requires a procedure of determining the singular-component contributions (or homogeneous solutions), either explicitly or implicitly. Through the intrinsic numerical computations, the SL93 scheme might have converged to a nonzero singular-component solution in a way different from what was implemented in the present UD retrievers.

4.4. *Optimal Spectral Resolutions*

We have made two high-resolution calculations for the vorticity retrievals in ET32 and OT32. The responses of tropical singularities, as measured by the wind and dynamics misfits, are greater in magnitude and shorter in length scale than those from the ET16 and OT16 runs, respectively. This can be attributed to the fact that the smallest nonzero eigenvalue decreases as the resolvable length scale decreases.

The optimal resolutions for retrieving the balanced winds appear to be between T12 and T18. High-resolution models tend to be not only subject to a higher degree of data contamination, but also more susceptible to the singularities. Low-resolution models, on the other hand, not only lack sufficient mode-to-mode couplings, but also are more likely to violate the end-mode conditions assumed in the FD and OD formulations.

4.5. *Singular Components in the Divergence Retrievals*

In the present study, the singular components are prescribed based upon a least-square fitting of the reanalysis wind data on the predetermined singular eigenmodes which are characterized by a peak(s) of normalized amplitude in the tropics. In the case of vorticity retrievals, the singular contributions are negligibly small (less than 3% of the global mean) due to the fact that the reanalysis vorticity distribution is highly orthogonal to the singular eigenfunction. The resulting well-fitting retrievals reflect the fact that NCEP uses the LBE as a constraint in its SSI data assimilation technique (Parrish and Derber [22].)

In contrast, the reanalysis divergence field exhibits a widespread, intense circulation pattern in the tropics as well as in the northern hemispheric subtropics. Thus, both symmetric and antisymmetric parts of the singular components play an important role in determining the divergence retrievals over the entire globe. Note that the actual impacts of the prescribed singular components are more complicated than the vorticity retrievals, due to the nonlinear interactions with the existing vorticity field during the functional iteration procedure. Without singular components, the resulting divergence and dynamics misfits would be unacceptably large.

In the future, the singular components for the divergence retrievals would be computed based upon the projection of a different estimate of divergence field that is less dependent upon the reanalysis data and the physics parameterizations therein. We are in the process of developing a variational approach to compute a vertical divergence profile which best fits the satellite's derived diabatic heating subject to various vertical integral constraints such as conservation of mass (as in O'Brien [15]), humidity, etc. The new divergence retrievals would then incorporate the information on the tropical convective heating, in addition to the nonlinear vorticity interaction.

5. CONCLUSIONS

The fact that the balance equations can be mathematically singular at or near the equator has long been recognized. A legitimate and perhaps more constructive and challenging question to ask is whether the singularity is removable and how to obtain a physically meaningful retrieval. In this paper, we retrieve the two kinds of balanced winds in the same generalized inverse problem. Our goal is to retrieve a balanced wind which best fits the observed wind while maintaining a weak constraint with the required balance conditions.

To facilitate a better understanding of the present inverse method, the retrievals were obtained by the generalized inverses of the kernel systems, which can be FD, OD, or UD depending upon how the spectral series are truncated.

The FD retrievers give rise to the strongest response to the tropical singularities. Although the retrieved winds exactly satisfy the LBE, they are not realistic and the information obtained is useless in practice. The OD retrievers significantly reduce the singularity responses but may induce a relatively large residual depending upon the resolution and quality of data that define the source function. The UD retrievers yield no response to the singularities but result in a pseudo residual. The UD retrievals are not unique; they vary depending on whether the eigenmodes include a scale-dependent weight and the quality of data used to compute the singular components. In this paper, we prescribed the singular components based upon the reanalysis wind data.

Realistic balanced winds along with small pseudo residuals are generally obtainable by the UD2 retrievers when an intermediate spectral resolution (T12–T18) is used and the singular components are included.

The usefulness of the wind retrievals from the balance models depends on the methodology selected to optimally control the effects of tropical singularities and to reduce the resulting residuals at the same time. Our numerical approach, which incorporates the generalized inversion techniques, illuminates the fundamental nature of the problem and provides a guideline for future improvements.

APPENDIX A

Variational Analyses for the Constrained Linear Inversion

The constrained linear inversion (e.g., Twomey [16]) seeks, among all possible solutions of ψ that minimizes the error of the LBE, the smoothest one as measured by its variance. The variational equation reads:

$$\delta \int \{(\nabla \cdot \mu \nabla \psi - q)^2 + \gamma \psi^2\} d\lambda d\mu = 0, \quad (\text{A1})$$

where γ is an undetermined Lagrangian multiplier. When γ is set to zero, i.e., as a nonconstrained linear inverse problem, the above variational equation reduces to the least-squares formulation of Baer [3].

In this paper we adapt a variant of the constrained linear inversion model with the smoothness of the solutions measured in terms of enstrophy, namely,

$$\delta \int \{(\nabla \cdot \mu \nabla \psi - q)^2 + \gamma \zeta^2\} d\lambda d\mu = 0. \quad (\text{A2})$$

Upon expanding the dependent variables in a series of spherical harmonic functions, employing the recursion relations of the associated Legendre polynomials as well as the spectral relation between ψ and ζ , we rewrite the above variational equation for given m as

$$\delta \int \left\{ \left(\sum_{j=0}^J \zeta_j H_j + \sum_{j=0}^J q_j P_j \right)^2 + \gamma \left(\sum_{j=0}^J \zeta_j P_j \right)^2 \right\} d\mu = 0, \quad (\text{A3})$$

where

$$H_j = a_j P_{j-1} + b_j P_{j+1}, \quad (\text{A4})$$

with a_j and b_j defined in (6) and (7). The outcome of the minimization procedure yields the traditional Galerkin formulation (e.g., Fletcher [23]), with the weight function H_j chosen from the same family (as linear combinations) of the trial function P_j . After evaluating the normalization integrals, the following system of normal equations emerges:

$$a_j b_{j-2} \zeta_{j-2} + (a_j^2 + b_j^2 + \gamma) \zeta_j + a_{j+2} b_j \zeta_{j+2} = (a_j q_{j-1} + b_j q_{j+1}). \quad (\text{A5})$$

It is important to note that the above system of equations is valid up to $j = J - 1$. The last equation in each linear system governing ζ_{j-2} and ζ_j would vary depending upon the choice of truncation that defines H_j . In the case of even truncation, $b_j = 0$ due to the truncation limit. Then, the equation at $j = J$ reduces to the same form as the kernel equation (4), assuming $\gamma = 0$.

If the variational equation in (A1) is used, then the normal equations are

$$\hat{a}_j \hat{b}_{j-2} \psi_{j-2} + (\hat{a}_j^2 + \hat{b}_j^2 - \gamma_\psi) \psi_j + \hat{a}_{j+2} \hat{b}_j \psi_{j+2} = -(\hat{a}_j q_{j-1} + \hat{b}_j q_{j+1}), \quad (\text{A6})$$

where $\hat{a}_j = a_j c_j$ and $\hat{b}_j = b_j c_j$. The above equation is identical with (20) of Baer [3] when γ_ψ is set to zero.

ACKNOWLEDGMENTS

The authors are indebted to W. Koshak for bringing the inversion techniques to their attention and for providing insightful discussion which led to the completion of this paper. This research was supported by the NASA Earth System Enterprise Office. Lu's work was supported by the Universities Space Research Association under NASA Cooperative Agreement NCC8-142. Programming assistance by J. Srikishen and information on the use of the NCEP/NCAR reanalysis data provided by Kanamitsu are greatly appreciated.

REFERENCES

1. E. Eliassen and B. Machenhauer, A study of the fluctuations of the atmospheric flow patterns represented by spherical harmonics, *Tellus* **17**, 220 (1965).
2. P. E. Merilees, On the linear balance equation in terms of spherical harmonics, *Tellus* **20**, 200 (1968).
3. F. Baer, The spectral balance equation, *Tellus* **29**, 107 (1977).
4. A. Wiin-Nielsen, On normal mode linear initialization on the sphere, *J. Atmos. Sci.* **36**, 2040 (1979).
5. R. Daley, Linear non-divergent mass-wind laws on the sphere, *Tellus* **35a**, 17 (1983).
6. R. Daley, *Atmospheric Data Analysis* (Cambridge Univ. Press, Cambridge, UK, 1991), p. 457.
7. G. J. Haltiner and R. T. Williams, *Numerical Prediction and Dynamic Meteorology* (Wiley, New York, 1980), p. 477.
8. S. Schubert, R. Rood, and J. Pfendtner, An assimilated dataset for earth sciences applications, *Bull. Am. Met. Soc.* **74**, 2331 (1993).
9. E. Kalnay, M. Kanamitsu, R. Kistler, W. Collins, D. Deaven, L. Gandin, M. Iredel, S. Saha, G. White, J. Woollen, Y. Zhu, M. Chelliah, W. Ebisuzaki, W. Higgins, J. Janowiak, K. Mo, C. Ropelewski, J. Wang, A. Leetmaa, R. Reynolds, R. Jenne, and D. Joseph, The NCEP/NCAR 40-years reanalysis project, *Bull. Am. Met. Soc.* **77**, 437 (1996).
10. P. D. Sardeshmukh and B. J. Hoskins, On the derivation of the divergent flow from the rotational flow: The χ problem, *Q. J. R. Met. Soc.* **113**, 339 (1987).
11. P. D. Sardeshmukh, The baroclinic χ problem and its application to the diagnosis of atmospheric heating rates, *J. Atmos. Sci.* **50**, 1099 (1993).
12. P. D. Sardeshmukh and B. Liebmann, An assessment of low-frequency variability in the tropics as indicated by some proxies of tropical convection, *J. Climate* **6**, 569 (1993).
13. K. Mo and E. M. Rasmusson, The 200-mb climatological vorticity budget during 1986–1989 as revealed by NMC analyses. *J. Climate* **6**, 577 (1993).
14. M. Newman, P. D. Sardeshmukh and J. W. Bergman, An assessment of the NCEP, NASA and ECMWF reanalyses over the tropical west Pacific warm pool, *Bull. Am. Met. Soc.* **81**, 41 (2000).
15. J. O'Brien, Alternative solutions to the classical vertical velocity problem, *J. Appl. Met.* **9**, 197 (1970).
16. S. Twomey, *Introduction to the Mathematics of Inversion in Remote Sensing and Indirect Measurements*. (Dover, New York, 1977), p. 243.
17. B. Noble and J. W. Daniel, *Applied Linear Algebra*, 3rd ed. (Prentice Hall, New York, 1988), p. 521.
18. J. J. Tribbia and R. A. Madden, Projection of time-mean geopotential heights onto normal, Hough modes, *Met. Atmos. Phys.* **38**, 9 (1988).
19. F. B. Hildebrand, *Methods of Applied Mathematics* (Prentice Hall, New York, 1965), p. 362.
20. B. Machenhauer, in *Numerical methods Used in Atmospheric Models*, GARP Publication Series No. 17, (World Meteorological Organization, Geneva) Vol. II, p. 124.
21. M. Kanamitsu and S. Saha, Systematic tendency error in budget calculations, *Mon. Wea. Rev.* **124**, 1145 (1996).
22. D. F. Parrish and J. C. Derber, The national meteorological center's spectral statistical-interpolation analysis system, *Mon. Wea. Rev.* **120**, 1747 (1992).
23. C. A. J. Fletcher, *Computational Galerkin Methods* (Springer-Verlag, Berlin/New York, 1984), p. 309.